Angiogenesis (2019) 22:237–250
https://doi.org/10.1007/s10456-018-9653-2

ORIGINAL PAPER

ADAM10 controls the differentiation of the coronary arterial endothelium

Gregory Farber[1] · Matthew M. Parks[1] · Nicole Lustgarten Guahmich[1] · Yi Zhang[2] · Sébastien Monette[3] · Scott C. Blanchard[1,4] · Annarita Di Lorenzo[2] · Carl P. Blobel[1,5,6]

Received: 25 October 2018 / Accepted: 8 November 2018 / Published online: 16 November 2018

Abstract

The coronary vasculature is crucial for normal heart function, yet much remains to be learned about its development, especially the maturation of coronary arterial endothelium. Here, we show that endothelial inactivation of ADAM10, a key regulator of Notch signaling, leads to defects in coronary arterial differentiation, as evidenced by dysregulated genes related to Notch signaling and arterial identity. Moreover, transcriptome analysis indicated reduced EGFR signaling in *A10ΔEC* coronary endothelium. Further analysis revealed that *A10ΔEC* mice have enlarged dysfunctional hearts with abnormal myocardial compaction, and increased expression of venous and immature endothelium markers. These findings provide the first evidence for a potential role for endothelial ADAM10 in cardioprotective homeostatic EGFR signaling and implicate ADAM10/Notch signaling in coronary arterial cell specification, which is vital for normal heart development and function. The ADAM10/Notch signaling pathway thus emerges as a potential therapeutic target for improving the regenerative capacity and maturation of the coronary vasculature.

Keywords Coronary vasculature · Endothelial Cells · ADAM10 (a disintegrin and metalloprotease 10) · Notch · Arterial differentiation

Introduction

Coronary circulation is crucial for supplying oxygen and nutrients to the heart and is therefore essential for the proper functioning of this vital organ. Since coronary artery disease is a major cause of mortality and morbidity, accounting for one in seven deaths in the United States [1], this provides a strong incentive to learn more about the development and homeostatic maintenance of the coronary vasculature. A better understanding of these processes has the long-term potential to help design improved approaches for repair or regeneration of diseased coronary vessels. The first steps of coronary vascular development are initiated by de novo vasculogenesis by endothelial progenitor populations originating in the endocardium and the sinus venosus [2–7]. This gives rise to vascular plexuses that develop into specific regions of the coronary vasculature in the endocardial or epicardial aspects of the heart [2, 3, 8]. As part of this process, the immature coronary endothelial cells differentiate into coronary veins, arteries, and capillaries. A recent single-cell analysis of coronary artery development identified vein-like arterial precursor cells and delineated several

Electronic supplementary material The online version of this article (https://doi.org/10.1007/s10456-018-9653-2) contains supplementary material, which is available to authorized users.

✉ Carl P. Blobel
blobelc@hss.edu

1 Department of Physiology, Biophysics and Systems Biology, Weill Cornell Medicine, New York, NY, USA

2 Center for Vascular Biology, Department of Pathology and Laboratory Medicine, Weill Cornell Medicine, New York, NY, USA

3 Laboratory of Comparative Pathology, Hospital for Special Surgery, Memorial Sloan Kettering Cancer Center, The Rockefeller University, Weill Cornell Medicine, New York, NY, USA

4 Tri-Institutional Training Program in Chemical Biology, Weill Cornell Medicine, New York, NY, USA

5 Arthritis and Tissue Degeneration Program, Hospital for Special Surgery, S-Building, Room 702, 535 East 70th Street, New York, NY 10021, USA

6 Institute for Advanced Study, Technical University Munich, Munich, Germany

steps along a gradual transition to arterial differentiation, yet much remains to be learned about the signaling mechanisms that promote the final steps in the development of mature coronary arterial endothelial cells [9].

The cell surface metalloprotease ADAM10 (a disintegrin and metalloprotease 10) is an essential regulator of physiological ligand-induced Notch signaling [10] and deletion of ADAM10 in endothelial cells results in defects in organ-specific vascular beds in mice, including the coronary vasculature, the developing retinal vasculature, the liver sinusoidal vessels, the glomeruli of the kidney, and the bone vasculature [11]. These vascular defects can be recapitulated by inactivating Notch1 in endothelial cells and Notch4 systemically (*N1ΔEC/N4−/−*), corroborating that the primary signaling pathway regulated by endothelial ADAM10 is the Notch pathway [12]. Endothelial cells have been shown to mainly express Notch1 and Notch4 as well as the ligands Dll4 and Jagged1 [13–15]. Proper heart development requires both Dll4- and Jag1-mediated Notch signaling [7, 16], and deletion of components of the Notch pathway result in heart valve malformations, aberrant coronary artery formation, and embryonic lethality [7, 11, 12, 16, 17]. Since *A10ΔEC* mice resemble *N1ΔEC/N4−/−* mice [11, 12], *A10ΔEC* animals provide a unique opportunity to examine the consequences of inactivating input from Notch signaling into coronary endothelial cells, regardless of the Notch ligand(s) or cell type activating this signaling.

Notch signaling is known to mediate arterial differentiation in the embryo [18] and in the yolk sac [19], raising questions about the role of this signaling pathway in arterial differentiation of the coronary vasculature. Therefore, the main goal of the current study was to examine the coronary vasculature in *A10ΔEC* mice to learn more about the contribution of ADAM10 to the development of coronary vessels and to determine whether it could be involved in arterial maturation. First, we performed histopathological, functional, and immunofluorescence analyses to better understand how the inactivation of ADAM10 affects the differentiation and function of the heart. Transcriptome-wide gene expression analysis with RNA-seq on enriched coronary endothelial cells from *A10ΔEC* mice revealed the contribution of ADAM10 to the coronary angiogenesis expression program in these cells. We contextualized these results by comparing them with previously reported studies on mice with mutations in other components of the Notch signaling pathway (e.g., Jag1 or 2, Dll4, mind bomb [16, 20, 21]). Since ADAM10 also cleaves other membrane proteins beside the Notch receptors, we asked whether the lack of processing of other known substrates of ADAM10 might become apparent through pathway analysis of the differentially expressed genes. Our results provide the first evidence, to our knowledge, for a homeostatic role of endothelial ADAM10 in protective EGFR signaling in the heart and they suggest that ADAM10 controls the final steps of arterial differentiation in mouse coronary vessels.

Results

A10ΔEC mice display abnormal myocardial compaction

Previous studies identified defects in the coronary vasculature of adult *A10ΔEC* mice [11], raising questions about how this affects the myocardium and whether any defects are also present earlier, at birth. Analysis of the H&E-stained sections from 6-week-old animals revealed an abnormal myocardial compaction with dilated capillaries in the outer parts of the myocardium of *A10ΔEC* animals compared to controls (Fig. 1a–d). Structural defects in the myocardium were also present in several newborn animals (P0), which displayed abnormal myocardial compaction (see Fig. 1e compared to 1f, representative for 2 out of 4 mutant animals) as well as enlarged dilated capillaries in the myocardium that were not evident in controls (Fig. 1g, h, CD31 stained sections shown in Fig. 1i, j, arrows indicate enlarged vessels in panels h and j). However, newborn animals did not appear to have the enlarged sub-epicardial vessels that are present in adult animals [11] (Fig. 1f). *A10ΔEC* hearts occasionally display regions of focal necrosis and calcification in adults (Suppl. Fig. 1a–c, 1 out of 2 mutant animals) and focal necrosis in newborn animals (Suppl. Fig. 1d, 2 out of 4 mutant animals). Previous studies have implicated Notch signaling in heart valve morphogenesis and myocardial compaction [12–15]. However, the aortic, pulmonary, and mitral valves of adult or newborn *A10ΔEC* mice had a comparable appearance to controls (representative adult aortic and mitral valves shown in Suppl. Fig. 2a–d, representative newborn aortic and pulmonary valves shown in Suppl. Fig. 2e–h).

A10ΔEC adult hearts display insufficient systolic contraction and are enlarged relative to body weight

Echocardiographic analysis of the hearts of *A10ΔEC* mice uncovered a 20% decrease in fractional shortening due to insufficient systolic ventricular contraction (Fig. 2a, b). These results provide the first direct evidence for a functional manifestation of the coronary endothelial abnormalities in *A10ΔEC* mice. In addition, the heart/body weight ratio in *A10ΔEC* mice was significantly increased (16.6%, SEM 4.5%) compared to control littermates (Fig. 2c, the mouse body and heart weights are shown separately in Suppl. Fig. 3a and b). Nevertheless, the echocardiographic measurements showed that the interventricular septal thickness, posterior wall thickness, and left ventricular mass

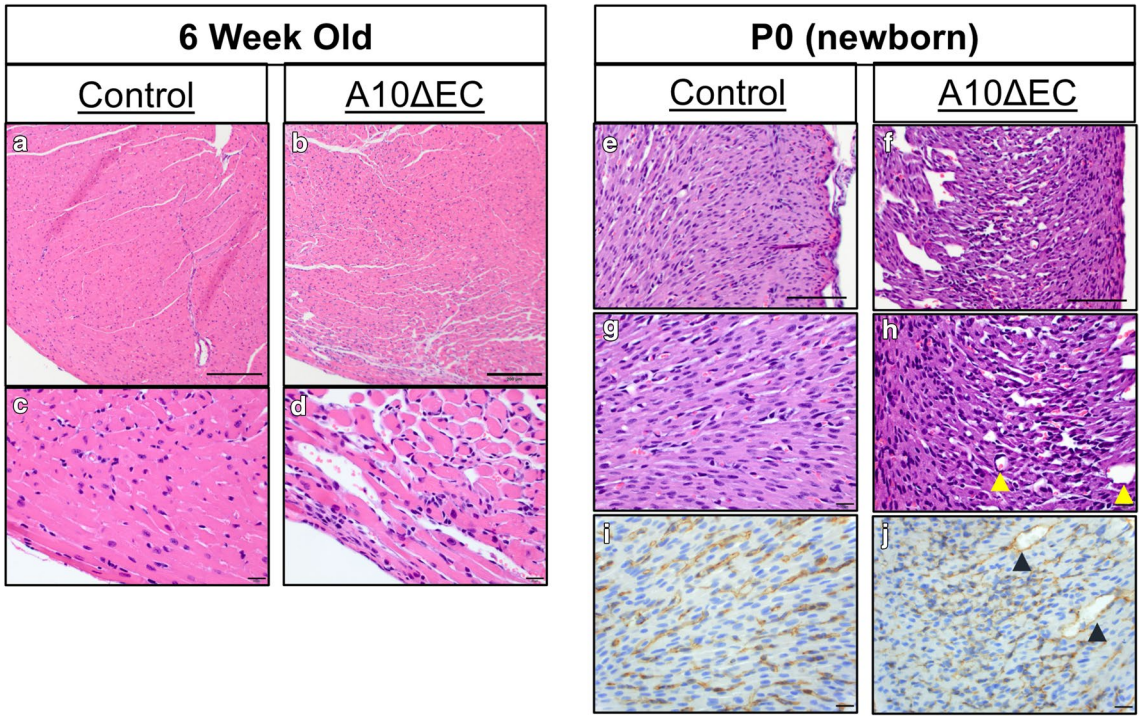

Fig. 1 *A10ΔEC* mice display abnormal myocardial compaction. H&E-stained sections of 6-week-old control (**a, c**) and mutant hearts (**b, d**) show abnormal myocardial compaction in the parts of the outer (epicardial) aspects of the myocardium in mutant *A10ΔEC* hearts (**b, d**) (parts of the left ventricular myocardium are shown in **a**–**d**). H&E-stained sections of newborn (P0) *A10ΔEC* hearts (**f, h**) also display abnormal myocardial compaction and contain enlarged myocardial capillaries (pointed by yellow arrows) when compared to control hearts (**e, g**). PECAM-stained sections show normal staining of myocardial capillaries in a control heart (**i**), but a less organized staining with some abnormally enlarged capillaries in a mutant *A10ΔEC* heart (pointed by black arrows **j**). Images are representative of sections of hearts from at least 3 separate animals per age and genotype. Scale bars **a, b** 200 µm, **c, d, g**–**j** 20 µm, **e, f** 100 µm

were comparable between mutant and control mice (Suppl. Fig. 3c–e). When we examined cardiomyocytes using fluorescent cell surface staining with wheat germ agglutinin (WGA) to identify possible hypo- or hypertrophy of these cells, we found that the cross-sectional area of cardiomyocytes in *A10ΔEC* animals was comparable to controls, arguing against cardiomyocyte hypertrophy as a cause for the enlarged hearts in these animals (Fig. 2d, e, quantification in f, see "Materials and methods" for details).

A10ΔEC mutant coronary vessels show higher endomucin expression and are Vegfr3 positive

To further characterize the coronary vasculature in *A10ΔEC* mice, we retro-orbitally injected a fluorescently tagged lectin to determine vascular perfusion (Fig. 3a, b). This demonstrated a comparable perfusion of the smaller myocardial vessels in *A10ΔEC* mice and controls. However, the abnormal sub-epicardial vessels that are found in *A10ΔEC* mice did not appear as well perfused as normal vessels (Fig. 3b, white arrows). Staining with anti-VEGFR2 antibodies showed a similar distribution of VEGFR2 positive vessels in mutant and control mice (Fig. 3c, d). Visualization of hypoxia in *A10ΔEC* hearts with hypoxyprobe revealed regions of hypoxia that were concentrated in the areas of abnormal compaction (Suppl. Fig. 4). Staining with alpha smooth muscle actin (α-SMA, Suppl. Fig. 5a) showed that most enlarged sub-epicardial vessels in *A10ΔEC* mice have a thin layer of mural cells, which is reminiscent of α-SMA staining of veins (white arrows in Suppl. Fig. 5a). Moreover, the ensheathment of larger arteries with α-SMA appeared comparable in *A10ΔEC* mice and controls (Suppl. Fig. 5b). Interestingly, the *A10ΔEC* coronary endothelium displayed stronger staining for endomucin, a marker of vein-like endothelium [22], compared to controls (Fig. 3e, f). The staining of the enlarged sub-epicardial vessels in *A10ΔEC* mice with anti-VEGFR3, but not with the lymphatic marker LYVE (Fig. 3g–l) indicates that they are not lymphatic vessels. This is of particular note since VEGFR3 is a marker of immature coronary endothelium [7] and VEGFR3 expression in control hearts overlaps partially with lymphatic vessels [23, 24] (Fig. 3k, l).

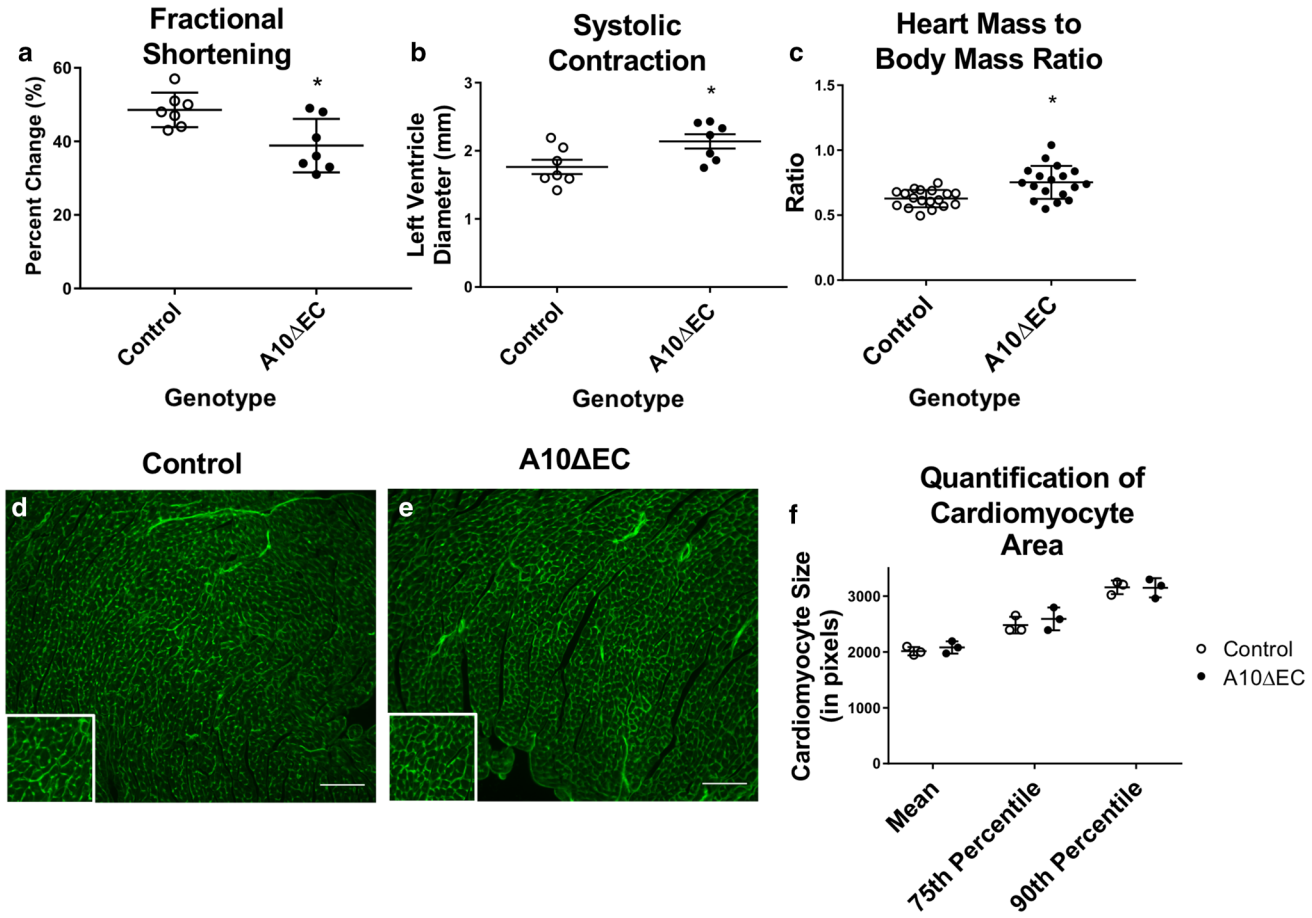

Fig. 2 *A10ΔEC* adult hearts are enlarged and display insufficient systolic contraction. *A10ΔEC* animals have decreased fractional shortening (**a**) and abnormal systolic contraction (**b**) relative to control animals ($n=7$ for each genotype, $p=0.012$). The ratio of heart mass relative to body mass in *A10ΔEC* mice is larger than in control animals (**c**) ($n=18$ for each genotype, $p=0.0008$). Representative images of adult cardiomyocytes stained with the lectin Wheat Germ Agglutinin (WGA) from control (**d**) and *A10ΔEC* animals (**e**). The images in **d, e** are representative of sections of hearts from three animals per genotype. The average mean cross-sectional area covered by individual myocardial cells, as well as the 75th percentile and 90th percentile area of these measurements for WGA-stained control and *A10ΔEC* cardiomyocytes was comparable (**f**, see Materials and methods for details). Scale bars 100 µm

RNA-seq of enriched *A10ΔEC* coronary endothelial cells shows immature arterial identity, evidence for cardiomyopathy, and altered Notch signaling

To learn more about potential changes in the transcriptional signature of coronary vessels from *A10ΔEC* mice, we performed RNA-seq on poly A-captured mRNA from coronary endothelial cells enriched from 6-week-old mutant animals and littermate controls. This uncovered 701 differentially expressed genes (428 upregulated and 273 downregulated, FDR < 0.05, Fig. 4a), including several genes that are involved in Notch signaling (Hey1, Smad6, Gja4, and Notch4). Hey1 and Smad6 were downregulated in *A10ΔEC* samples, corroborating the synergism between Smad6 and Notch signaling [18]. Interestingly, Notch4 was upregulated in *A10ΔEC* samples, perhaps to compensate for the lack of ADAM10/Notch1 signaling. In addition, we observed lower expression of VEGFR1 as well as VEGFb and VEGFc, the latter of which is known to have a role in coronary artery and capillary growth [1, 19]. Moreover genes that are considered to be markers for arterial endothelium were downregulated (Gja4, Igfbp3, and Hey1). We also found that the Apelin receptor (Aplnr) was upregulated in *A10ΔEC* samples, as previously observed in glomerular endothelial cells isolated from these animals [20]. In addition, we noted a differential regulation of tetraspanin14 (Tspan14), an ADAM10-interacting protein that could potentially be involved in regulating ADAM10-dependent processing of Notch receptors [22]. Finally, components of several disease and signaling pathways were significantly enriched for in differentially expressed genes (Fig. 4b). The most prominent pathways were those seen in dilated cardiomyopathy, hypertrophic cardiomyopathy, cGMP/PKG signaling (involved in Calcium signaling), and vascular smooth muscle contraction [25].

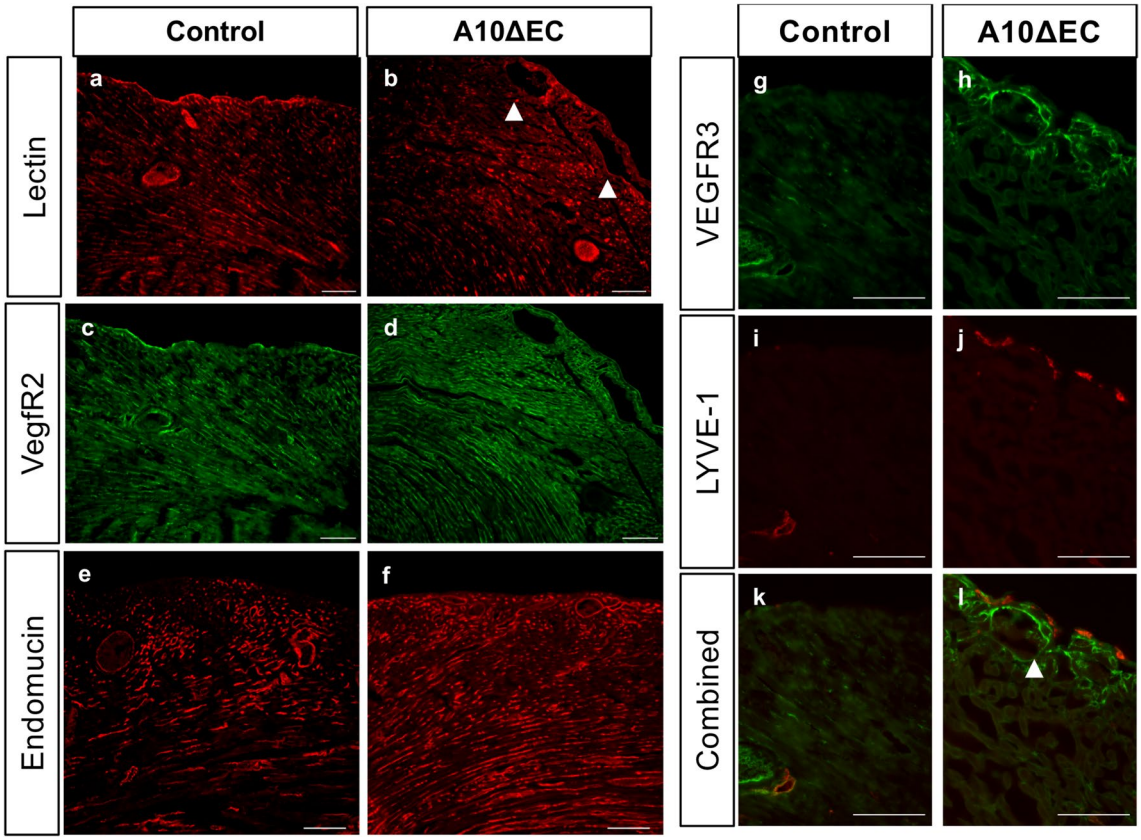

Fig. 3 Evaluation of perfusion and endothelial cell identity markers in *A10ΔEC* hearts. **a, b** The lectin perfusion of myocardial vessels in *A10ΔEC* animals appears similar to that of control animals. However, the abnormally enlarged sub-epicardial vessels (white arrows) did not appear to be as well perfused as normal vessels. **c, d** Vegfr2 staining is comparable in an *A10ΔEC* heart relative to a control. **e, f** *A10ΔEC* hearts have higher and more uniform levels of endomucin staining throughout the epicardium and myocardium. **g, h** The abnormal and enlarged sub-epicardial vessels in *A10ΔEC* mice stain with VEGFR3, a marker for immature arterial endothelial cells, but not LYVE, a marker for lymphatic vessels (**i, j**), merged images in **k, l**. Each image is representative of sections from at least 3 separate animals per genotype. Scale bars: 100 µm

LINCS analysis provides evidence for dysregulated EGFR signaling in *A10ΔEC* mice

ADAM10 has several other substrate proteins besides Notch [26, 27], including the EGFR ligands BTC and EGF [28, 29] and the amyloid precursor protein [30]. We were therefore interested in determining whether other signaling pathways, which do not directly depend on Notch signaling, might be affected in *A10ΔEC* endothelial cells. When we entered the 701 differentially regulated genes into the LINCS database (http://www.lincsproject.org/), split into upregulated and downregulated genes, we found a highly significant overlap with gene sets that are dysregulated in tumor cells treated with ligands of the EGF-receptor (EGFR), such as betacellulin (BTC), TGFα (TGFA), EGF, and epiregulin (EPR) (Fig. 4c). Since all of these ligands can activate the EGFR (ErbB1), these results provide evidence for a possible dysregulation of the EGFR signaling pathway in *A10ΔEC* endothelial cells. Moreover, these findings are consistent with the known role of ADAM10 as the primary sheddase of BTC and EGF [28, 31]. Interestingly, two of the three other signaling protein-dependent pathways implicated in this comparison (Gas6, and HRG) rely on receptors that can be shed by ADAM10 (the Gas6 receptor Axl [32] and the HRG receptor c-Met [33]).

Comparison of gene sets dysregulated in *A10ΔEC* to other Notch pathway mutants

ADAM10 is a critical regulator of physiological ligand-induced Notch signaling (reviewed in [10]), and the vascular phenotype of *A10ΔEC* mice resembles that of *Notch1ΔEC/Notch4−/−* mice [11, 12]. We therefore compared the *A10ΔEC* coronary endothelial gene set to gene expression measurements from mice lacking other components of the Notch signaling pathway in endothelial cells or in other cell types in the heart [13, 24], as well as with models for heart development and disease (Fig. 5a) [25].

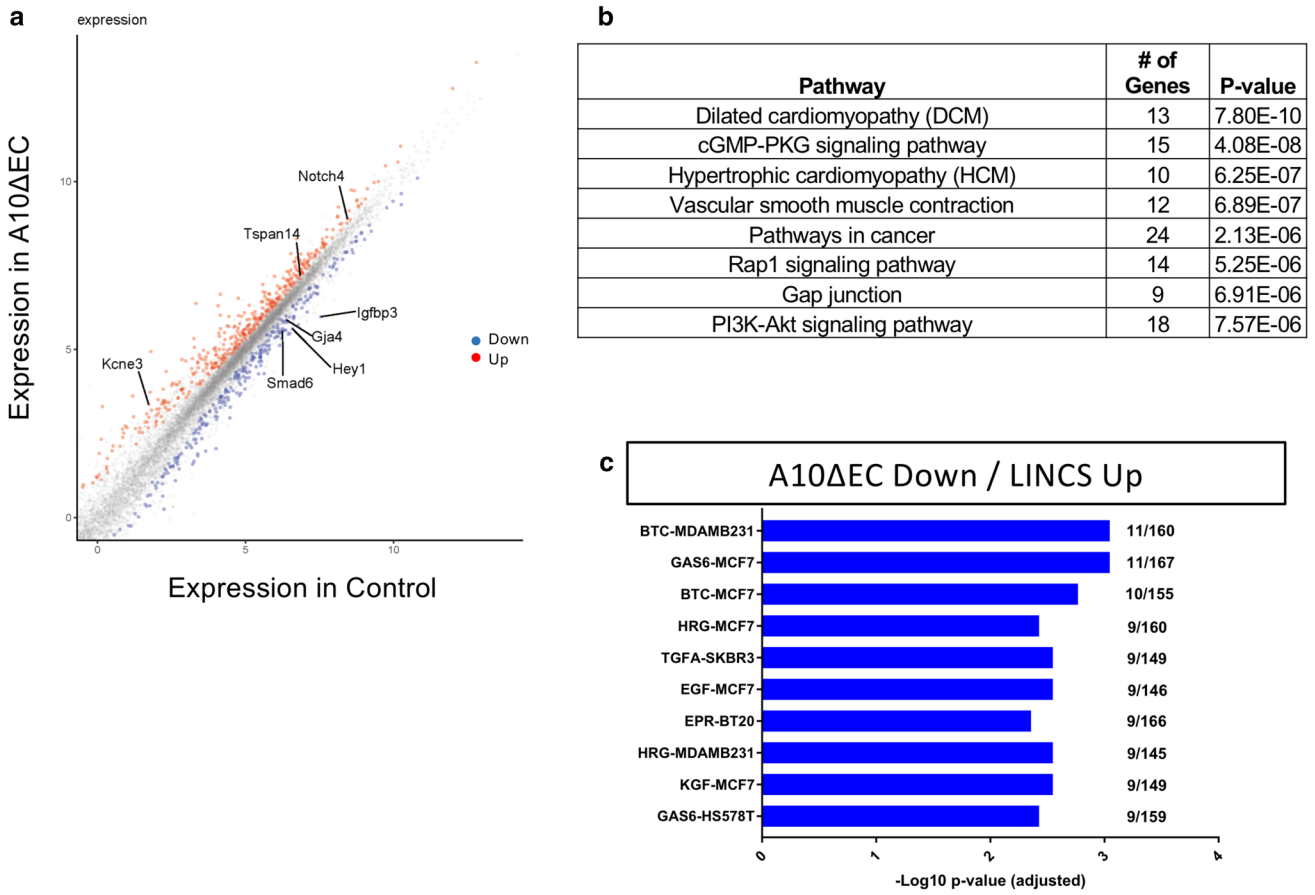

Pathway	# of Genes	P-value
Dilated cardiomyopathy (DCM)	13	7.80E-10
cGMP-PKG signaling pathway	15	4.08E-08
Hypertrophic cardiomyopathy (HCM)	10	6.25E-07
Vascular smooth muscle contraction	12	6.89E-07
Pathways in cancer	24	2.13E-06
Rap1 signaling pathway	14	5.25E-06
Gap junction	9	6.91E-06
PI3K-Akt signaling pathway	18	7.57E-06

Fig. 4 *A10ΔEC* heart endothelial cells differentially express genes related to Notch signaling and cardiomyopathies. **a** Scatterplot of 701 differentially expressed genes. Select genes related to the Notch signaling pathway are highlighted. **b** Top pathways found to be dysregulated in *A10ΔEC* coronary endothelial cells compared to controls by Kyoto Encyclopedia of Genes and Genomes (KEGG) analysis. **c** Top 10 enriched gene sets found when the *A10ΔEC* data set was compared to the Library of Integrated Network-Based Cellular Signatures (LINCS l1000) database

Importantly, we took the direction of change of the differentially expressed genes into account when assessing the similarity with other gene sets (see "Materials and methods" for details). The highest level of similarity with the *A10ΔEC* coronary endothelial gene set was with developing heart endothelial cells, consistent with a role for ADAM10/Notch signaling in promoting the maturation of coronary endothelial cells. In addition, there was a significant overlap of the *A10ΔEC* coronary endothelial gene signature with that of L-type relative to H-type endothelial cells in bone [21]. Since ablation of endothelial Notch signaling results in more L-type endothelial cells in bone at the expense of H-type cells [17, 24, 26], this suggests that these different Notch-dependent endothelial cell fate decisions share at least some common underlying features (Fig. 5a).

When we compared the *A10ΔEC* RNA-seq data set with results from other studies on Notch signaling in the heart, we found significant similarity with data from mice in which the Notch ligand Dll4 was inactivated by a pan-endothelial deletion (Tie2-Cre) or endocardial deletion (Nfatc-Cre) et E9.5 (Fig. 5a) [16]. The differentially expressed genes observed upon deletion of Dll4 with Tie2-Cre are more similar with the *A10ΔEC* gene set than with data from endocardial cells lacking Dll4. Moreover, when compared to the *A10ΔEC* data set, the genes affected by Notch1 deletion in the endocardium are not as similar as those affected by endocardial deletion of Dll4, consistent with our previous finding that endothelial deletion of Notch1 and deletion of Notch4 is required to recapitulate the full range of vascular phenotypes seen in *A10ΔEC* animals [9]. Knockout of manic fringe (Mfng) and mind bomb (Mibc) also resulted in similar differential gene expression when compared to the *A10ΔEC* gene set. Interestingly, the similarity to the data set with the cumulative effects of deleting the Notch ligands Jag1 and Jag2 in cardiomyocytes (cTNT-Cre) was stronger (16 genes similarly affected) than the comparison to data from individually

a

Mouse Model	P-value	Significant? (Y=*/N=Ø)	Total Gene Overlap	Overlap Up Genes	Overlap Down Genes
Developing Heart Endothelial Cells	1.0E-6	*	107	36	71
L-type to H-type Bone Endothelial Cells	6.0E-6	*	89	17	72
Dll4Tie2	0	*	67	48	19
Dll4Nfatc	3.5E-4	*	42	28	14
N1Nfatc	0.09	Ø	16	13	3
Mfng	0	*	66	41	25
MibcTnT	6E-6	*	21	5	16
Jag1/Jag2cTnT	0.016	*	16	15	1
Jag2cTnT	0.50	Ø	1	1	0
Jag1cTnT	0.53	Ø	2	1	1
Heart Endothelial Cells Post Myocardial Infarct	0.084	Ø	12	12	0

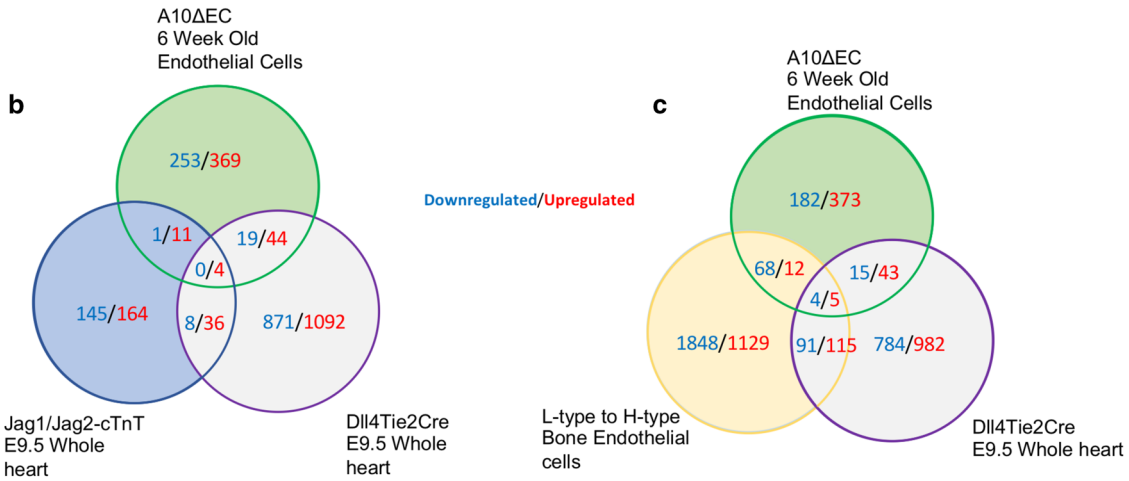

d

Gene	Direction	Comparison
Adora2a	Up	A10 to Dll4Tie2Cre to Jag1Jag2
Kcne3	Up	A10 to Dll4Tie2Cre to Jag1Jag2
Glul	Up	A10 to Dll4Tie2Cre to Jag1Jag2
Gramd1b	Up	A10 to Dll4Tie2Cre to Jag1Jag2
Gmfg	Up	A10 to Dll4Tie2Cre to Bone
Gmfg	Up	A10 to Dll4Tie2Cre to Developing Heart
Gja4	Down	A10 to Dll4Tie2Cre to Bone
Gramd1b	Up	A10 to Dll4Tie2Cre to Bone

Fig. 5 *A10ΔEC* gene set enrichment analysis compared to other mouse models. **a** *A10ΔEC* differentially expressed genes compared to other published gene sets derived from mutations that affect different components of the Notch signaling pathway, $*p < 0.05$. **b** Venn diagram comparison of *A10ΔEC* to *Dll4-Tie2Cre* and *Jag1Jag2cTnT* data sets [16]. **c** Venn diagram comparison of data from *A10ΔEC* to *Dll4-Tie2Cre* and to genes enriched in L-type versus H-type bone endothelium [21]. **d** Summary of overlapping genes from **b, c**

deleting Jag1 or 2 (only 3 genes similarly affected when combined), suggesting a partial functional redundancy of Jag1 and 2 with respect to activating ADAM10-dependent Notch signaling in coronary endothelial cells. Finally, the overlap with differentially expressed genes in isolated endothelial cells from hearts following a myocardial infarct was not statistically significant, consistent with the notion that the *A10ΔEC* phenotype is mostly likely developmental or chronic in nature, but not acute.

Identification of common transcriptional changes in selected data sets

Jagged and Delta-like4 have been implicated in different aspects of Notch signaling in retinal endothelial cells, with Dll4 implicated in tip-stalk cell signaling, and Jagged1 in modulating the interaction between Dll4 and Notch [34, 35]. Since inactivation of ADAM10 in coronary endothelial cells should block input from these two structurally and functionally different Notch ligands [36, 37], we compared

the differentially expressed genes from all three analyses to identify dysregulated genes that they have in common. Such genes could serve as markers of ADAM10/Notch-dependent endothelial cell fate decisions. Out of the four genes uncovered in this analysis (Fig. 5b), Adora2a, Kcne3, Glul, and Gramd1b, the first two are consistent with defects in Notch signaling. Specifically, Adora2a is involved in pathological neovascularization [27], whereas Kcne3 is a marker for tip cells [38]. In addition, we found that Gmfg was upregulated in the *A10ΔEC, Dll4-Tie2Cre*, Bone Vasculature, and Developing Heart data sets (Fig. 5c, d, Suppl. Fig. 6A). Gmfg is linked to tip cells [28] and blood islands found in developing yolk sacs [29]. Gja4, a known arterial marker and Notch target gene [39], is one of the nine genes present in the L-type to H-type, *Dll4-Tie2Cre*, and *A10ΔEC* data sets (Fig. 5d).

Finally, we wanted to determine whether the gene expression profile after inactivation of Dll4 in the endocardium (*Dll4-NfatcCre*) is similar to the gene expression profile of the coronary endothelium in *A10ΔEC* mice (*A10-Tie2Cre*) and Dll4-Tie2Cre mice. Using the *A10ΔEC* data set as a point of comparison, we first analyzed the genes that are only found in the *Dll4-Tie2Cre* and *A10ΔEC* data sets, but not in the *Dll4-NfatcCre* data set, based on the assumption that the latter is more representative of endocardially derived endothelial cells. We found 44 differentially expressed genes (12 downregulated and 32 upregulated), including Gmfg and AplnR receptor, which can be considered potential markers for ADAM10/Notch signaling in the epicardial coronary vasculature. (Suppl. Fig. 6B). Finally, 23 differentially expressed genes (7 downregulated and 16 upregulated) were found in all three gene sets, including the known Notch signaling targets, Adora2a, Kcne3, and Gja4.

Discussion

The premise for this study was our previous observation that inactivation of ADAM10 in endothelial cells results in the development of abnormal coronary vessels [11]. To learn more about the nature of these defects and their underlying causes, we performed a histopathological and functional analysis of the hearts of *A10ΔEC* mice and a transcriptional analysis of coronary endothelium from these animals. The functional studies uncovered a reduction in fractional shortening of *A10ΔEC* hearts, providing the first evidence that their coronary vascular abnormalities have functional consequences. The general perfusion of the heart, as assessed by lectin staining, seemed normal, although the coronary vasculature in CD31-stained sections had a different appearance in the mutant animals. The presence of areas of hypoxia and, in some cases, focal necrosis in the mutant hearts could provide an explanation, at least in part, for the reduced fractional shortening, which could be further exacerbated by the lack of myocardial compaction in the sub-epicardial aspect in *A10ΔEC* hearts.

Our gene expression analysis revealed that the *A10ΔEC* coronary endothelial cells displayed a transcriptional profile resembling that of endothelial cells in developing hearts. This suggests that ADAM10/Notch signaling is important for the maturation of the coronary endothelium. Recent studies have shown that coronary endothelial cells are initially vein-like, and then differentiate through a series of steps into arterial and venous vessels [7]. The transcription factor COUP-TFII is crucial for the first step of differentiation of veins from the coronary vascular progenitors, but the final steps towards arterial differentiation have not yet been fully defined. Our observations that arterial markers (e.g., Gja4, Hey1, Igfbp3) are downregulated in *A10ΔEC* coronary endothelia relative to controls support the notion that ADAM10-Notch-dependent signaling promotes the acquisition of the mature coronary arterial cell fate (see Fig. 6). Additionally, the presence of VEGFR3-positive enlarged vessels in the sub-epicardial portion of mature *A10ΔEC* hearts further serves as an indicator that these vessels contain immature coronary arterial cells, and potentially coronary angiogenic precursors [7].

ADAM10 is crucial for activating Notch signaling in cis, i.e., in the same cell that is expressing a given ligand-activated Notch receptor [40, 41]. Consequently, inactivating ADAM10 in endothelial cells should block the input from ligand-induced canonical Notch signaling into these cells, regardless of the ligand or cell type providing the input. This notion is supported by the significant overlap with differentially expressed genes from mice lacking other components of the Notch signaling pathway in coronary endothelial cells or in other cell types in the heart. Specifically, inactivation

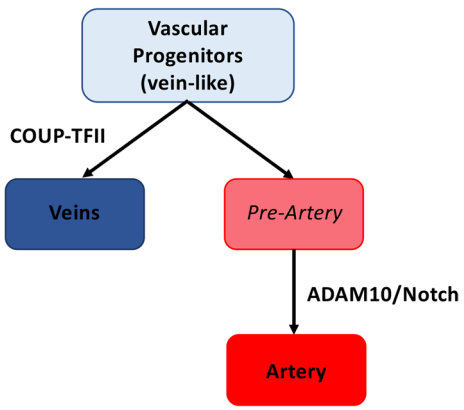

Fig. 6 Schematic of artery–vein specification of coronary endothelium. Coronary progenitor cells originating from the sinus venosus and endocardium first undergo a cell fate decision, regulated by COUP-TFII, to become veins or pre-arterial cells. The full differentiation of pre-arterial cells into mature arterial endothelium requires ADAM10-dependent canonical Notch signaling

of the Notch ligand Dll4 in endothelial cells affected several of the same genes as inactivation of ADAM10. In addition, targeting both Notch ligands Jagged1 and 2 in cardiomyocytes also resulted in transcriptional changes that significantly overlapped with those observed in *A10ΔEC* mice, but had almost no overlap in Dll4 mutant mice. Thus, different ligands can apparently elicit distinct ADAM10-dependent Notch signals. Presumably, this can be explained by differences in the spatiotemporal expression of different Notch ligands as well as by the context provided by the differentiation states of the signal-receiving cells. On the other hand, four genes were similarly affected in *A10ΔEC* as in mice carrying mutations in Dll4 or Jag1/2, two of which are known to have prominent roles in Notch signaling and tip/stalk cell fate decisions (Kcne3 and Adora2a) [38, 42]. These results suggest that the inactivation of ADAM10 in endothelial cells also affects a limited number of common genes that respond to ligand-induced Notch signaling, regardless of the ligand. Thus, inactivation of ADAM10 in endothelial cells apparently represents an efficient approach to inactivate canonical Notch signaling in these cells.

ADAM10 is known to have numerous other substrates besides the Notch receptors, including the amyloid precursor protein and the EGFR ligands BTC and EGF [26–30]. Nevertheless, Notch is considered to be a principal substrate of ADAM10, at least during mouse development, since almost all of the developmental phenotypes caused by inactivation of ADAM10 signaling can be explained by the resulting lack of Notch signaling (reviewed in [10]). It was therefore interesting to find that *A10ΔEC* endothelial cells showed gene expression signatures consistent with defects in EGFR signaling. Ligands of the EGFR, such as BTC, EGF, or TGFα, are made as membrane-anchored precursors that must be processed, typically by ADAM10 or the related ADAM17, to activate the EGFR (reviewed in [31]). Most phenotypes of mice lacking ADAM17 can be attributed to a defect in EGFR signaling [43–47], which is consistent with the essential role of ADAM17 in processing several EGFR ligands, including TGFα, HB-EGF, and Amphiregulin [43–45]. However, as noted above, two out of the seven known ligands of the EGFR, BTC, and EGF, are preferentially processed by ADAM10 [28, 29], which is consistent with a possible role for ADAM10 in cardiac EGFR signaling. Interestingly, EGFR inhibitors used to treat cancer can cause cardiomyopathy [48–50], providing further support to the notion that EGFR signaling is cardioprotective. These results are thus the first to suggest a possible role of ADAM10 in protective EGFR signaling in the heart, most likely through the release of EGF or BTC, which have been reported to be expressed in endothelial cells (Bend3 [51]). However, we cannot rule out possible indirect effects of ADAM10 on EGFR signaling, e.g., through a Notch-dependent process that affects other components of the EGFR signaling pathway.

ADAM10/Notch signaling-dependent endothelial cell fate decisions are known to be crucial for the development of organ-specific vascular beds, such as in the glomerular and bone endothelium [17, 20]. The mature glomerular and coronary vasculature is thought to derive from progenitor cells that arise from outside the main vascular tree and must undergo vasculogenesis in order to generate these specialized vascular structures (reviewed in [10]). This is conceptually similar to the vasculogenesis events that represent the first steps of vascular development in the yolk sac or in the embryo, which require Notch signaling [10, 18]. Interestingly, the expression of Gmfg, a marker of the blood islands of the developing yolk sac [29], is increased in both the heart and bone endothelium in *A10ΔEC* mice, further supporting the notion that there is an impediment in vascular maturation in these specialized vascular niches. On the other hand, there are also key differences in the dysregulated genes in different vascular beds of *A10ΔEC* mice, presumably because of the specific requirements of the final differentiation state of a given organ. An example is provided by glomerular endothelial cells [52], where ADAM10/Notch signaling regulates the formation of glomerular fenestrae and the vascular morphology of glomerular tufts [20]. Notch signaling also mediates the transition from L-type to H-type bone endothelium, which is crucial to long bone growth [24]. In the case of the coronary endothelium, the results presented here support a model in which ADAM10/Notch signaling controls the final maturation of arterial endothelial cells (Fig. 6). The inability of the coronary arteries to mature properly in *A10ΔEC* mice correlates with abnormal myocardial compaction, enlarged heart mass relative to body mass as well as heart dysfunction, illustrating the importance of the differentiation of arterial coronary endothelium for normal heart development and function.

Providing a better understanding of the cellular signaling pathways involved in the maturation of the coronary vascular network is crucial to understanding cardiac development and to help uncover new approaches for harnessing the regenerative potential of the coronary endothelium. In addition, studies on the differentiation of coronary vessels have the potential to elucidate the homeostatic signaling provided by fully differentiated coronary endothelial cells in normal and pathologic states [53]. This study indicates that the modulation of the endothelial ADAM10/Notch signaling pathway could be a potential tool for future therapeutic approaches to promote arterial differentiation in coronary disease and organ regeneration. Furthermore, our data suggest that ADAM10 plays a crucial role in the acquisition of organ-specific endothelial identity in several distinct vascular structures, warranting future investigations into the common themes that unite these unique vascular beds.

Materials and methods

Immunofluorescence reagents

The antibodies against VEGFR3 (goat anti-mouse, R&D Systems (Minneapolis, MN) #AF743) and VEGFR2 (goat anti-mouse, R&D Systems #AF644) were used at a 1:50 dilution; the anti-LYVE (rabbit anti-mouse Abcam, (Cambridge, MA) #ab14917) was used at 1:250; the anti-αSMA (mouse anti-mouse Dako, (Santa Clara, CA) #M0851) was used at 1:100, and anti-PECAM/CD31 antibody (rat monoclonal, catalog #DIA-310; Dianova, Hamburg, Germany) was used at 1:250. Secondary antibodies were Donkey anti-rabbit 594 (#21207 Thermo Fisher, Grand Island, NY); Donkey anti-goat 488 (Abcam #ab150129); Donkey anti-goat 546 (Thermo Fisher #A11056); and Donkey anti-mouse 488 (Abcam #ab150105) were all used at a dilution of 1:250. Sections from a total of three pairs of *A10ΔEC* mice and littermate controls were analyzed per antibody, with at least one pair of littermates of each gender.

Mice

The *A10ΔEC* mouse strain used here has been previously described [52]. Adult female mice of mixed genetic background (129 Sv/C57Bl6) carrying two floxed alleles of ADAM10 were mated with male mice carrying two floxed alleles of ADAM10 and one allele of the Tie2-Cre transgene [54]. Male or female offspring from such a mating containing two alleles of floxed ADAM10 and one allele of the Tie2-Cre transgene were referred to as *A10ΔEC* mice, whereas littermates with two floxed alleles of ADAM10, but no Tie2-Cre, were used as controls. All experiments were performed with gender-matched littermate male or female mice, as indicated. All procedures were approved by the Animal Care and Use Committee of Weill Cornell Medicine.

Histopathologic examination

Hearts were fixed by immersion in 10% neutral buffered formalin, processed routinely in alcohol and xylene, embedded in paraffin, sectioned at 5-micron thickness, and stained with hematoxylin and eosin. Sections were examined and images prepared by a board-certified veterinary pathologist (SM). Sections from a total of 2 pairs of *A10ΔEC* mice and littermate controls were analyzed for 6-week-old mice, and 4 pairs for newborn (P0) mice.

Chromogenic immunohistochemistry

Chromogenic immunohistochemistry for PECAM-1 (CD31) on formalin fixed paraffin embedded sections was performed on a Leica Bond RX automated staining platform (Leica Biosystems). Following heat-induced epitope retrieval at pH 9.0, the primary antibody was applied at a concentration of 1:250 and was followed by application of a rabbit anti-rat secondary antibody, mouse adsorbed (Vector Laboratories BA-4001), and a polymer detection system (Novocastra Bond Polymer Refine Detection, Leica Biosystems). The chromogen was 3,3 diaminobenzidine tetrachloride (DAB), and sections were counterstained with haematoxylin. Sections were examined and images prepared by a board-certified veterinary pathologist (SM). Sections from a total of four pairs of newborn (P0) *A10ΔEC* mice and littermate controls were analyzed.

Echocardiogram

Echocardiography was performed on 6-week-old adult mice using the Vevo 770 Imaging system (VisualSonics, Toronto, Canada). The mice were anesthetized using isoflurane, and measurements were collected for 3–6 consecutive cycles, as previously described [55]. In short, left ventricle contraction (diastolic (LVd) and systolic dimensions (LVs)) was measured using data collected in M-mode traces. Fractional shortening was calculated by the following equation: $([LVd - LVs]/LVd \times 100)$. A total of 14 mice were analyzed (7 control and 7 *A10ΔEC*); each *A10ΔEC* mutant animal was matched to a littermate.

Retro-orbital injection

Mice were anesthetized with isoflurane and then injected retro-orbitally with 100 µl of a lectin solution (for 1 ml, 900 µl PBS and 100 µl *Lycopersicon esculentum* tomato lectin (Vector Labs #DL-1178)), left in a cage for 10 min and then sacrificed so that the tissues could be prepared for further analysis.

Immunofluorescence

The hearts were fixed in 4% paraformaldehyde overnight at 4 °C, then dehydrated in 15% sucrose followed by 30% sucrose overnight. The tissue was then frozen and sectioned at 12 µm. Slides with frozen heart sections were incubated in blocking solution (1% donkey serum (Jackson ImmunoResearch, West Grove, PA) in 0.5% Triton X-100 and 0.1% Saponin in PBS (TSP)) for 1 h at 37 °C. Slides were then treated with primary antibodies in blocking solution for 1 h at 37 °C. Next, slides were washed in TSP three times for 5 min at room temperature, then

treated with secondary antibodies in blocking solution for 1 h at 37 °C. After the staining with secondary antibodies, the slides were washed 3x in TSP for five minutes each at room temperature and mounted with Prolong Diamond solution (Thermo Fisher #P36965) and a coverslip. The images were collected on a Nikon Ni-E microscope with an Andor Zyla camera. All images were analyzed using either Nikon NIS Elements or ImageJ software.

Hypoxyprobe

Three pairs of 6-week-old adult mice (2 male pairs and 1 female pair) were injected with 60 mg/kg of Hypoxyprobe solution via intraperitoneal injection. After 1 h, the mice were sacrificed, their hearts isolated and then fixed with 4% PFA overnight. The hearts were dehydrated with 15% and 30% sucrose overnight, then frozen, and sectioned with a thickness of 12 µm. The resulting sections were blocked and then stained with Hypoxyprobe-Red549 at a dilution of 1:200 (Hypoxyprobe #HP7-100kit, Hypoxyprobe, Burlington, MA).

Isolation of coronary endothelial cells

Mice were sacrificed with CO_2 following the guidelines of the American Veterinary Association. Mouse hearts were collected and washed in PBS to remove excess blood. Samples were then minced into small pieces and moved to a 50-ml Falcon tube, digested in 3 ml solution consisting of 1 mg/ml Collagenase Type II (Sigma #C6885, St. Louis, MO), 1 ml of Dispase (Stemcell #07923, Cambridge, MA), and 1 ml PBS. Samples were digested for an hour at 37 °C and resuspended and mixed with a pipette after 30 and 60 min. The dissociated tissue was then filtered through a 70-µm mesh sieve (Corning #352350, Corning, NY) and washed three times with PBS. The suspension was spun down in a centrifuge for 8 min at 200×*g*, then the supernatant removed, and the pellet resuspended in PBS, followed by a second identical washing step. The final pellet was resuspended in 1 ml wash buffer (PBS with 0.5% BSA and 2 mM EDTA) and moved to a 5-ml round bottom Falcon tube. Magnetic Dynabeads (Thermo Fisher #11035) with coupled Pecam antibodies (BD Biosciences #553370, Sparks, MD) were added to the resuspended pellet, and the suspension left on a rotating incubator for 40 min at 4 °C. The beads with bound cells were isolated using a Dynal magnet and washed five times to remove loosely bound cells while the tube was still attached to the magnet. The RNA from the isolated cells was purified using an RNeasy isolation kit (Qiagen #74104, Germantown, MD).

RNA sequencing

Library preparation and RNA sequencing was performed on six samples from three control and three *A10ΔEC* animals (a total of 3 pairs of gender-matched littermates from different litters, 2 male pairs, and 1 female pair) by the Weill Cornell Genomic Core Facility. The libraries were prepared using TruSeq Stranded mRNA Library Prep (poly A selection; Illumina #20020594, San Diego, CA). The sequencing was performed on an Illumina HiSeq4000 with 50 bp single-end reads.

RNA sequencing data analysis

Raw sequencing reads were aligned to the GRCm38 reference genome with STAR [56]. Gene expression was quantified with RSEM [57]. Differential expression was assessed with limma using voom with observations weights [58]. Kyoto Encyclopedia of Genes and Genomes (KEGG) pathway [59] enrichment was determined with the Fisher's exact test. Permutation tests were performed to test for statistically significant overlaps between two differentially expressed gene sets. In particular, for $i = 1$, 2 consider differentially expressed gene set S_i consisting of $n_{u,i}$ upregulated genes and $n_{d,i}$ downregulated genes. The aim is to test if the total number of commonly regulated genes between S_1 and S_2, i.e., upregulated in both S_1 and S_2 or downregulated in both S_1 and S_2, is higher than expected by chance. For $n = 10^6$ permutations, we sampled $n_{u,2}$ genes and $n_{d,2}$ genes and counted the total number overlapping genes by comparing to those upregulated and downregulated in gene set S_1, respectively. All RNA-seq data has been deposited to the Sequence Read Archive under BioProject PRJNA504649.

Quantification of cardiomyocyte area

Frozen sections of adult heart (12 µm) were stained with fluorescently tagged wheat germ agglutinin (Sigma #L4895). The stained tissues were then imaged, with three images per animal. Each image was of a section from a different region of the heart (ranging from the apex to base). Regions were isolated from the images of the left ventricle and subjected to the morphological segmentation plugin in MorphoLibJ (ImageJ) to record the area of the segmented cardiomyocytes using the measure particle feature. Only the smallest cross-sectional areas of the measured cardiomyocytes were used in statistical analysis. These values were screened from the obtained data set by solely analyzing cardiomyocytes whose longest dimension was only twice the shortest dimension. A total of three 6-week-old male littermate pairs were

analyzed, each consisting of one *A10ΔEC* and one control animal.

Statistical analysis

A two-tailed *t* test performed with GraphPad Prism 7 was used to measure statistical significance. *p* values of 0.05 or less were regarded as statistically significant.

Acknowledgements We thank the Weill Cornell Genomics core for their contribution to the RNA-seq analysis presented here. In addition, we would like to thank Chad Kurylo for his insightful comments and suggestions. This study was funded in part by NIH GM64750 to CPB. G. Farber is funded by American Heart Association Predoctoral Fellowship (#17PRE33380001). S. Monette and the Laboratory of Comparative Pathology was supported in part by NCI Grant P30 CA008748. A. di Lorenzo was supported by NIH NHLBI R01HL126913 and NINDS R21NS104512.

Author contributions GF and CB designed the experiments and prepared the manuscript. GF harvested all tissue and maintained the mouse colony. GF performed immunofluorescence experiments and analyses. MP performed the RNA-seq analysis. GF and NLG prepared the samples for RNA sequencing. YZ performed the echocardiogram experiments. SM analyzed and collected images for histopathology analysis. AdL and SB provided resources and relevant feedback. All authors contributed to the editing of the manuscript.

Compliance with ethical standards

Conflict of interest The authors declare that they have no conflict of interest.

References

1. Benjamin EJ, Blaha MJ, Chiuve SE, Cushman M, Das SR, Deo R, de Ferranti SD, Floyd J, Fornage M, Gillespie C, Isasi CR, Jimenez MC, Jordan LC, Judd SE, Lackland D, Lichtman JH, Lisabeth L, Liu S, Longenecker CT, Mackey RH, Matsushita K, Mozaffarian D, Mussolino ME, Nasir K, Neumar RW, Palaniappan L, Pandey DK, Thiagarajan RR, Reeves MJ, Ritchey M, Rodriguez CJ, Roth GA, Rosamond WD, Sasson C, Towfighi A, Tsao CW, Turner MB, Virani SS, Voeks JH, Willey JZ, Wilkins JT, Wu JH, Alger HM, Wong SS, Muntner P, American Heart Association Statistics Committee and Stroke Statistics Subcommittee (2017) Heart disease and stroke statistics—2017 update: a report from the American Heart Association. Circulation 135(10):e146–e603. https://doi.org/10.1161/CIR.0000000000000485
2. Chen HI, Sharma B, Akerberg BN, Numi HJ, Kivela R, Saharinen P, Aghajanian H, McKay AS, Bogard PE, Chang AH, Jacobs AH, Epstein JA, Stankunas K, Alitalo K, Red-Horse K (2014) The sinus venosus contributes to coronary vasculature through VEGFC-stimulated angiogenesis. Development 141(23):4500–4512. https://doi.org/10.1242/dev.113639
3. Luttun A, Carmeliet P (2003) De novo vasculogenesis in the heart. Cardiovasc Res 58(2):378–389
4. Tian X, Hu T, Zhang H, He L, Huang X, Liu Q, Yu W, He L, Yang Z, Zhang Z, Zhong TP, Yang X, Yang Z, Yan Y, Baldini A, Sun Y, Lu J, Schwartz RJ, Evans SM, Gittenberger-de Groot AC, Red-Horse K, Zhou B (2013) Subepicardial endothelial cells invade the embryonic ventricle wall to form coronary arteries. Cell Res 23(9):1075–1090. https://doi.org/10.1038/cr.2013.83
5. Tian X, Pu WT, Zhou B (2015) Cellular origin and developmental program of coronary angiogenesis. Circ Res 116(3):515–530. https://doi.org/10.1161/CIRCRESAHA.116.305097
6. Wu B, Zhang Z, Lui W, Chen X, Wang Y, Chamberlain AA, Moreno-Rodriguez RA, Markwald RR, O'Rourke BP, Sharp DJ, Zheng D, Lenz J, Baldwin HS, Chang CP, Zhou B (2012) Endocardial cells form the coronary arteries by angiogenesis through myocardial-endocardial VEGF signaling. Cell 151(5):1083–1096. https://doi.org/10.1016/j.cell.2012.10.023
7. Wang Y, Wu B, Lu P, Zhang D, Wu B, Varshney S, Del Monte-Nieto G, Zhuang Z, Charafeddine R, Kramer AH, Sibinga NE, Frangogiannis NG, Kitsis RN, Adams RH, Alitalo K, Sharp DJ, Harvey RP, Stanley P, Zhou B (2017) Uncontrolled angiogenic precursor expansion causes coronary artery anomalies in mice lacking Pofut1. Nat Commun 8(1):578. https://doi.org/10.1038/s41467-017-00654-w
8. Red-Horse K, Ueno H, Weissman IL, Krasnow MA (2010) Coronary arteries form by developmental reprogramming of venous cells. Nature 464(7288):549–553. https://doi.org/10.1038/nature08873
9. Su T, Stanley G, Sinha R, D'Amato G, Das S, Rhee S, Chang AH, Poduri A, Raftrey B, Dinh TT, Roper WA, Li G, Quinn KE, Caron KM, Wu S, Miquerol L, Butcher EC, Weissman I, Quake S, Red-Horse K (2018) Single-cell analysis of early progenitor cells that build coronary arteries. Nature 559(7714):356–362. https://doi.org/10.1038/s41586-018-0288-7
10. Alabi RO, Farber G, Blobel CP (2018) Intriguing roles for endothelial ADAM10/Notch signaling in the development of organ-specific vascular beds. Physiol Rev 98(4):2025–2061. https://doi.org/10.1152/physrev.00029.2017
11. Glomski K, Monette S, Manova K, De Strooper B, Saftig P, Blobel CP (2011) Deletion of Adam10 in endothelial cells leads to defects in organ-specific vascular structures. Blood 118(4):1163–1174. https://doi.org/10.1182/blood-2011-04-348557
12. Alabi RO, Glomski K, Haxaire C, Weskamp G, Monette S, Blobel CP (2016) ADAM10-dependent signaling through Notch1 and Notch4 controls development of organ-specific vascular beds. Circ Res 119(4):519–531. https://doi.org/10.1161/CIRCRESAHA.115.307738
13. Krebs LT, Xue Y, Norton CR, Shutter JR, Maguire M, Sundberg JP, Gallahan D, Closson V, Kitajewski J, Callahan R, Smith GH, Stark KL, Gridley T (2000) Notch signaling is essential for vascular morphogenesis in mice. Genes Dev 14(11):1343–1352
14. del Monte G, Casanova JC, Guadix JA, MacGrogan D, Burch JB, Perez-Pomares JM, de la Pompa JL (2011) Differential Notch signaling in the epicardium is required for cardiac inflow development and coronary vessel morphogenesis. Circ Res 108(7):824–836. https://doi.org/10.1161/CIRCRESAHA.110.229062
15. MacGrogan D, D'Amato G, Travisano S, Martinez-Poveda B, Luxan G, Del Monte-Nieto G, Papoutsi T, Sbroggio M, Bou V, Gomez-Del Arco P, Gomez MJ, Zhou B, Redondo JM, Jimenez-Borreguero LJ, de la Pompa JL (2016) Sequential ligand-dependent Notch signaling activation regulates valve primordium formation and morphogenesis. Circ Res 118(10):1480–1497. https://doi.org/10.1161/CIRCRESAHA.115.308077
16. D'Amato G, Luxan G, del Monte-Nieto G, Martinez-Poveda B, Torroja C, Walter W, Bochter MS, Benedito R, Cole S, Martinez F, Hadjantonakis AK, Uemura A, Jimenez-Borreguero LJ, de la Pompa JL (2016) Sequential Notch activation regulates ventricular chamber development. Nat Cell Biol 18(1):7–20. https://doi.org/10.1038/ncb3280
17. Luxan G, D'Amato G, MacGrogan D, de la Pompa JL (2016) Endocardial Notch signaling in cardiac development and

disease. Circ Res 118(1):e1–e18. https://doi.org/10.1161/CIRCRESAHA.115.305350
18. Kim YH, Hu H, Guevara-Gallardo S, Lam MT, Fong SY, Wang RA (2008) Artery and vein size is balanced by Notch and ephrin B2/EphB4 during angiogenesis. Development 135(22):3755–3764. https://doi.org/10.1242/dev.022475
19. Copeland JN, Feng Y, Neradugomma NK, Fields PE, Vivian JL (2011) Notch signaling regulates remodeling and vessel diameter in the extraembryonic yolk sac. BMC Dev Biol 11:12. https://doi.org/10.1186/1471-213X-11-12
20. Quaife-Ryan GA, Sim CB, Ziemann M, Kaspi A, Rafehi H, Ramialison M, El-Osta A, Hudson JE, Porrello ER (2017) Multicellular transcriptional analysis of mammalian heart regeneration. Circulation 136(12):1123–1139. https://doi.org/10.1161/CIRCULATIONAHA.117.028252
21. Langen UH, Pitulescu ME, Kim JM, Enriquez-Gasca R, Sivaraj KK, Kusumbe AP, Singh A, Di Russo J, Bixel MG, Zhou B, Sorokin L, Vaquerizas JM, Adams RH (2017) Cell-matrix signals specify bone endothelial cells during developmental osteogenesis. Nat Cell Biol 19(3):189–201. https://doi.org/10.1038/ncb3476
22. dela Paz NG, D'Amore PA (2009) Arterial versus venous endothelial cells. Cell Tissue Res 335(1):5–16. https://doi.org/10.1007/s00441-008-0706-5
23. Tammela T, Zarkada G, Wallgard E, Murtomaki A, Suchting S, Wirzenius M, Waltari M, Hellstrom M, Schomber T, Peltonen R, Freitas C, Duarte A, Isoniemi H, Laakkonen P, Christofori G, Yla-Herttuala S, Shibuya M, Pytowski B, Eichmann A, Betsholtz C, Alitalo K (2008) Blocking VEGFR-3 suppresses angiogenic sprouting and vascular network formation. Nature 454(7204):656–660. https://doi.org/10.1038/nature07083
24. Kaipainen A, Korhonen J, Mustonen T, van Hinsbergh VW, Fang GH, Dumont D, Breitman M, Alitalo K (1995) Expression of the fms-like tyrosine kinase 4 gene becomes restricted to lymphatic endothelium during development. Proc Natl Acad Sci USA 92(8):3566–3570
25. Carvajal JA, Germain AM, Huidobro-Toro JP, Weiner CP (2000) Molecular mechanism of cGMP-mediated smooth muscle relaxation. J Cell Physiol 184 (3):409–420. https://doi.org/10.1002/1097-4652(200009)184:3%3C409::AID-JCP16%3E3.0.CO;2-K
26. Kuhn PH, Colombo AV, Schusser B, Dreymueller D, Wetzel S, Schepers U, Herber J, Ludwig A, Kremmer E, Montag D, Muller U, Schweizer M, Saftig P, Brase S, Lichtenthaler SF (2016) Systematic substrate identification indicates a central role for the metalloprotease ADAM10 in axon targeting and synapse function. eLife. https://doi.org/10.7554/eLife.12748
27. Weskamp G, Ford J, Sturgill J, Martin S, Docherty A, Swendeman S, Broadway N, Hartmann D, Saftig P, Umland S, Sehara-Fujisawa A, Black R, Ludwig A, Becherer D, Conrad D, Blobel C (2006) ADAM10 is a principal 'sheddase' of the low-affinity immunoglobulin E receptor CD23. Nat Immunol 7:1393–1298
28. Sahin U, Weskamp G, Zhou HM, Higashiyama S, Peschon JJ, Hartmann D, Saftig P, Blobel CP (2004) Distinct roles for ADAM10 and ADAM17 in ectodomain shedding of six EGFR-ligands. J Cell Biol 164:769–779
29. Sanderson MP, Erickson SN, Gough PJ, Garton KJ, Wille PT, Raines EW, Dunbar AJ, Dempsey PJ (2005) ADAM10 mediates ectodomain shedding of the betacellulin precursor activated by p-aminophenylmercuric acetate and extracellular calcium influx. J Biol Chem 280(3):1826–1837
30. Kuhn PH, Wang H, Dislich B, Colombo A, Zeitschel U, Ellwart JW, Kremmer E, Rossner S, Lichtenthaler SF (2010) ADAM10 is the physiologically relevant, constitutive alpha-secretase of the amyloid precursor protein in primary neurons. EMBO J 29(17):3020–3032. https://doi.org/10.1038/emboj.2010.167
31. Blobel CP (2005) ADAMs: key players in EGFR-signaling, development and disease. Nat Rev Mol Cell Biol 6:32–43
32. Miller MA, Sullivan RJ, Lauffenburger DA (2017) Molecular pathways: receptor ectodomain shedding in treatment, resistance, and monitoring of cancer. Clin Cancer Res 23(3):623–629. https://doi.org/10.1158/1078-0432.CCR-16-0869
33. Yang Y, Wang Y, Zeng X, Ma XJ, Zhao Y, Qiao J, Cao B, Li YX, Ji L, Wang YL (2012) Self-control of HGF regulation on human trophoblast cell invasion via enhancing c-Met receptor shedding by ADAM10 and ADAM17. J Clin Endocrinol Metab 97(8):E1390–E1401. https://doi.org/10.1210/jc.2012-1150
34. Blanco R, Gerhardt H (2013) VEGF and Notch in tip and stalk cell selection. Cold Spring Harb Perspect Med 3(1):a006569. https://doi.org/10.1101/cshperspect.a006569
35. Benedito R, Roca C, Sorensen I, Adams S, Gossler A, Fruttiger M, Adams RH (2009) The Notch ligands Dll4 and Jagged1 have opposing effects on angiogenesis. Cell 137(6):1124–1135. https://doi.org/10.1016/j.cell.2009.03.025
36. Luca VC, Kim BC, Ge C, Kakuda S, Wu D, Roein-Peikar M, Haltiwanger RS, Zhu C, Ha T, Garcia KC (2017) Notch-Jagged complex structure implicates a catch bond in tuning ligand sensitivity. Science 355(6331):1320–1324. https://doi.org/10.1126/science.aaf9739
37. Luca VC, Jude KM, Pierce NW, Nachury MV, Fischer S, Garcia KC (2015) Structural biology. Structural basis for Notch1 engagement of Delta-like 4. Science 347(6224):847–853. https://doi.org/10.1126/science.1261093
38. Zhao Q, Eichten A, Parveen A, Adler C, Huang Y, Wang W, Ding Y, Adler A, Nevins T, Ni M, Wei Y, Thurston G (2018) Single-cell transcriptome analyses reveal endothelial cell heterogeneity in tumors and changes following antiangiogenic treatment. Cancer Res 78(9):2370–2382. https://doi.org/10.1158/0008-5472.CAN-17-2728
39. Fang JS, Coon BG, Gillis N, Chen Z, Qiu J, Chittenden TW, Burt JM, Schwartz MA, Hirschi KK (2017) Shear-induced Notch-Cx37-p27 axis arrests endothelial cell cycle to enable arterial specification. Nat Commun 8(1):2149. https://doi.org/10.1038/s41467-017-01742-7
40. Groot AJ, Vooijs MA (2012) The role of Adams in Notch signaling. Adv Exp Med Biol 727:15–36. https://doi.org/10.1007/978-1-4614-0899-4_2
41. Kopan R, Ilagan MX (2009) The canonical Notch signaling pathway: unfolding the activation mechanism. Cell 137(2):216–233. https://doi.org/10.1016/j.cell.2009.03.045
42. Liu Z, Yan S, Wang J, Xu Y, Wang Y, Zhang S, Xu X, Yang Q, Zeng X, Zhou Y, Gu X, Lu S, Fu Z, Fulton DJ, Weintraub NL, Caldwell RB, Zhang W, Wu C, Liu XL, Chen JF, Ahmad A, Kaddour-Djebbar I, Al-Shabrawey M, Li Q, Jiang X, Sun Y, Sodhi A, Smith L, Hong M, Huo Y (2017) Endothelial adenosine A2a receptor-mediated glycolysis is essential for pathological retinal angiogenesis. Nat Commun 8(1):584. https://doi.org/10.1038/s41467-017-00551-2
43. Peschon JJ, Slack JL, Reddy P, Stocking KL, Sunnarborg SW, Lee DC, Russel WE, Castner BJ, Johnson RS, Fitzner JN, Boyce RW, Nelson N, Kozlosky CJ, Wolfson MF, Rauch CT, Cerretti DP, Paxton RJ, March CJ, Black RA (1998) An essential role for ectodomain shedding in mammalian development. Science 282:1281–1284
44. Jackson LF, Qiu TH, Sunnarborg SW, Chang A, Zhang C, Patterson C, Lee DC (2003) Defective valvulogenesis in HB-EGF and TACE-null mice is associated with aberrant BMP signaling. EMBO J 22(11):2704–2716
45. Sternlicht MD, Sunnarborg SW, Kouros-Mehr H, Yu Y, Lee DC, Werb Z (2005) Mammary ductal morphogenesis requires paracrine activation of stromal EGFR via ADAM17-dependent shedding of epithelial amphiregulin. Development 132(17):3923–3933

46. Franzke CW, Cobzaru C, Triantafyllopoulou A, Loffek S, Horiuchi K, Threadgill DW, Kurz T, van Rooijen N, Bruckner-Tuderman L, Blobel CP (2012) Epidermal ADAM17 maintains the skin barrier by regulating EGFR ligand-dependent terminal keratinocyte differentiation. J Exp Med 209(6):1105–1119. https://doi.org/10.1084/jem.20112258
47. Chalaris A, Adam N, Sina C, Rosenstiel P, Lehmann-Koch J, Schirmacher P, Hartmann D, Cichy J, Gavrilova O, Schreiber S, Jostock T, Matthews V, Hasler R, Becker C, Neurath MF, Reiss K, Saftig P, Scheller J, Rose-John S (2010) Critical role of the disintegrin metalloprotease ADAM17 for intestinal inflammation and regeneration in mice. J Exp Med 207(8):1617–1624. https://doi.org/10.1084/jem.20092366
48. Gronich N, Lavi I, Barnett-Griness O, Saliba W, Abernethy DR, Rennert G (2017) Tyrosine kinase-targeting drugs-associated heart failure. Br J Cancer 116(10):1366–1373. https://doi.org/10.1038/bjc.2017.88
49. Tang XM, Chen H, Liu Y, Huang BL, Zhang XQ, Yuan JM, He X (2017) The cardiotoxicity of cetuximab as single therapy in Chinese chemotherapy-refractory metastatic colorectal cancer patients. Medicine (Baltimore) 96(3):e5946. https://doi.org/10.1097/MD.0000000000005946
50. Monsuez JJ, Charniot JC, Vignat N, Artigou JY (2010) Cardiac side-effects of cancer chemotherapy. Int J Cardiol 144(1):3–15. https://doi.org/10.1016/j.ijcard.2010.03.003
51. Gomez-Gaviro MV, Scott CE, Sesay AK, Matheu A, Booth S, Galichet C, Lovell-Badge R (2012) Betacellulin promotes cell proliferation in the neural stem cell niche and stimulates neurogenesis. Proc Natl Acad Sci USA 109(4):1317–1322. https://doi.org/10.1073/pnas.1016199109
52. Farber G, Hurtado R, Loh S, Monette S, Mtui J, Kopan R, Quaggin S, Meyer-Schwesinger C, Herzlinger D, Scott RP, Blobel CP (2018) Glomerular endothelial cell maturation depends on ADAM10, a key regulator of Notch signaling. Angiogenesis. https://doi.org/10.1007/s10456-018-9599-4
53. MacGrogan D, Munch J, de la Pompa JL (2018) Notch and interacting signalling pathways in cardiac development, disease, and regeneration. Nat Rev Cardiol 15(11):685–704. https://doi.org/10.1038/s41569-018-0100-2
54. Kisanuki YY, Hammer RE, Miyazaki J, Williams SC, Richardson JA, Yanagisawa M (2001) Tie2-Cre transgenic mice: a new model for endothelial cell-lineage analysis in vivo. Dev Biol 230(2):230–242
55. Zhang Y, Huang Y, Cantalupo A, Azevedo PS, Siragusa M, Bielawski J, Giordano FJ, Di Lorenzo A (2016) Endothelial Nogo-B regulates sphingolipid biosynthesis to promote pathological cardiac hypertrophy during chronic pressure overload. JCI Insight. https://doi.org/10.1172/jci.insight.85484
56. Dobin A, Davis CA, Schlesinger F, Drenkow J, Zaleski C, Jha S, Batut P, Chaisson M, Gingeras TR (2013) STAR: ultrafast universal RNA-seq aligner. Bioinformatics 29(1):15–21. https://doi.org/10.1093/bioinformatics/bts635
57. Li B, Dewey CN (2011) RSEM: accurate transcript quantification from RNA-Seq data with or without a reference genome. BMC Bioinform 12:323. https://doi.org/10.1186/1471-2105-12-323
58. Liu R, Holik AZ, Su S, Jansz N, Chen K, Leong HS, Blewitt ME, Asselin-Labat ML, Smyth GK, Ritchie ME (2015) Why weight? Modelling sample and observational level variability improves power in RNA-seq analyses. Nucleic Acids Res 43(15):e97. https://doi.org/10.1093/nar/gkv412
59. Kanehisa M, Furumichi M, Tanabe M, Sato Y, Morishima K (2017) KEGG: new perspectives on genomes, pathways, diseases and drugs. Nucleic Acids Res 45(D1):D353–D361. https://doi.org/10.1093/nar/gkw1092